PHYSICAL REVIEW B **81**, 165422 (2010)

Topological metal at the surface of an ultrathin $Bi_{1-x}Sb_x$ alloy film

T. Hirahara,[1,*] Y. Sakamoto,[1] Y. Saisyu,[1] H. Miyazaki,[2] S. Kimura,[2] T. Okuda,[3,†] I. Matsuda,[3] S. Murakami,[4] and S. Hasegawa[1]

[1]*Department of Physics, University of Tokyo, 7-3-1 Hongo, Bunkyo-ku, Tokyo 113-0033, Japan*

[2]*UVSOR Facility, Institute for Molecular Science, Okazaki 444-8585, Japan*

[3]*Synchrotron Radiation Laboratory, ISSP, University of Tokyo, Kashiwa 277-8581, Japan*

[4]*Department of Physics, Tokyo Institute of Technology, Tokyo 152-8551, Japan*

(Received 28 January 2010; revised manuscript received 25 March 2010; published 15 April 2010)

We have studied the growth and electronic/transport properties of ultrathin $Bi_{1-x}Sb_x$ alloy films, which the bulk is reported to be a topological insulator for $0.07<x<0.22$. We found that single crystal epitaxial films as thin as ~30 Å could be grown on silicon for $0\leq x<0.32$. The Z_2 topological number of the films was shown to be nontrivial from the surface Fermi surface. Moreover a crossover from an insulating to a metallic behavior was observed upon reducing the film thickness, revealing the clear detection of the topological-metal conductivity. Our results settle the controversial issues concerning the metallicity of $Bi_{1-x}Sb_x$ at low temperature and verify that the surface/volume ratio must be extensively enhanced to properly understand the nature of these surface states.

DOI: 10.1103/PhysRevB.81.165422 PACS number(s): 71.18.+y, 71.70.Ej, 73.20.−r, 73.25.+i

Recently there has been growing interest in two-dimensional (2D) quantum spin Hall (QSH) systems or three-dimensional (3D) topological insulators (TI) both theoretically as well as experimentally.[1] Topological insulators are nonmagnetic insulators whose gap is generated by spin-orbit coupling but possess metallic edge modes (surface states). They are a novel topological phase characterized by the Z_2 topological number $(\nu_0;\nu_1\nu_2\nu_3)$, which can be calculated from the bulk band structure.[2] ν_0 is the most important, and for conventional insulators $\nu_0=0$ (trivial), while for TI $\nu_0=1$ (nontrivial). The intriguing nature of the surface states is that they are topologically protected and hence called *topological metals*; they are robust against disorder or modest changes of boundary conditions, such as nonmagnetic impurities or surface roughness.[3] Moreover, it has been predicted by theory that by placing ferromagnetic materials or superconductors in contact with TI, even more exotic physical phenomena such as magnetic monopoles[4] or Majorana Fermions[5] can be observed.

Up to now most of the experimental studies have been conducted for single crystal bulk materials such as $Bi_{1-x}Sb_x$ $(0.07<x<0.22)$,[6–8] Bi_2Se_3,[9] and Bi_2Te_3 (Ref. 10) using (spin- and) angle-resolved photoemission spectroscopy (ARPES). It can be expected that at very low temperatures, the bulk carriers will be frozen out and the surface-state properties will show up. But the problem with these bulk materials is that it is difficult to make them "insulating." For example, it was reported that some bulk bands cross the Fermi level due to the change of the Fermi level possibly due to Se/Te site defects in the latter two systems. Some attempts have been made to make them insulating by substituting Bi with Ca/Sn or depositing NO_2 on the surface,[11] but it is unknown whether such effects can be really regarded as a "weak perturbation." Recently, transport and magnetic measurements on $Bi_{1-x}Sb_x$ were performed.[12] They reported a change from an insulator to a conductor at low temperature, indicating the expected surface-state conductivity. However, it was shown that the metallicity was ascribed not only to the 2D states but also due to a 3D component by measuring the magnetic-field-dependent oscillations. This was explained as a result of a coupling of the surface and bulk states even though there was no indication of metallic bulk bands in ARPES. Although this coupling itself is intriguing, it is a pity that it might hinder the topological nature of the 2D edge states. One solution to the above problem is to enhance the surface/volume ratio by making a topological metal at the surface of an ultrathin film. Also the crossover from 3D TI to 2D QSH when the system size is reduced is now being investigated theoretically and gaining attention.[13]

In the present work, we have attempted to prepare a topological metal at the surface of an ultrathin film whose thickness is in the order of several ten angstroms. The growth of $Bi_{1-x}Sb_x$ on Si(111)-7×7 was monitored by reflection high-energy-electron diffraction (RHEED) and it was found that single crystal films as thin as ~30 Å can be fabricated. The Fermi surface of such films was mapped by ARPES and showed that the Z_2 topological number is "nontrivial." Furthermore, we found that the band gap of the ultrathin films is larger than that of the bulk crystal and the surface-state contribution dominates the film conductivity for the thinnest films. These results suggest that the conductivity of the topological metal has actually been detected and points to the importance of strongly enhancing the surface/volume ratio in investigating the nature of TI.

The temperature dependence of the electrical conductivity was measured *in situ* by monolithic micro four-point-probes (MFPP, probe spacing: 20 μm) in a custom-made ultrahigh vacuum chamber.[14] The ARPES experiments were performed at BL-5U of UVSOR using MBS-Toyama A-1 at 10 K and also at BL-18A of KEK-Photon Factory using VG-Scienta SES-100 at 100 K. First, a clean Si(111)-7×7 surface was prepared on an *n*-type substrate (P-doped, 1–10 Ω·cm) by a cycle of resistive heat treatments. Bi and Sb were co-deposited on the 7×7 surface at room temperature monitored by RHEED. The deposition rates of Bi and Sb were calibrated by the formation of $\sqrt{3}\times\sqrt{3}$ phases[15] and confirmed by the allotropic transformation in the case of Bi.[16] One bilayer (BL) is defined as the atomic density of the

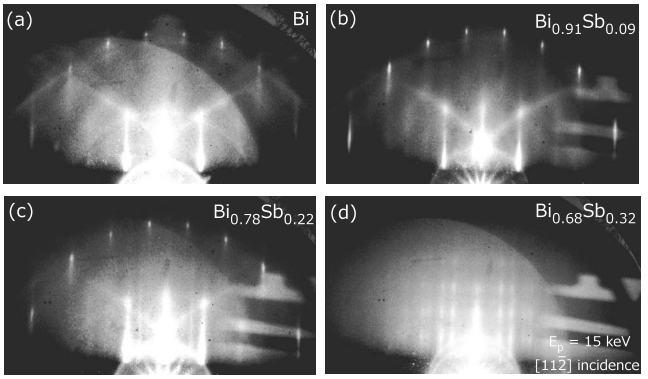

FIG. 1. RHEED patterns of 29 Å (7 BL) thick pure Bi (a), $Bi_{0.91}Sb_{0.09}$ (b), $Bi_{0.78}Sb_{0.22}$ (c), and 50 Å (13 BL) thick $Bi_{0.68}Sb_{0.32}$ (d) ultrathin films. The electrons are incident along the [11$\bar{2}$] direction and the energy is 15 keV.

Bi(001) plane, which is 1.14×10^{15} cm^{-2}(3.9 Å).

First, we have performed RHEED observations to check whether a single-crystalline $Bi_{1-x}Sb_x$ film can be formed on a Si substrate. It is known that epitaxial ultrathin Bi films as thin as 25 Å can be prepared on Si(111)-7×7 by deposition at room temperature.[16] Figure 1(a) shows the RHEED pattern of a 29 Å (7 BL) thick Bi film. The 1×1 periodicity can clearly be seen with Kikuchi patterns representing the good crystalline quality. Figure 1(b) shows the RHEED pattern of a 7 BL thick $Bi_{0.91}Sb_{0.09}$ film which Bi and Sb were codeposited at the ratio of approximately 10:1. No noticeable change in the in-plane lattice constant was observed within the experimental resolution. The general features of Figs. 1(b) and 1(c) ($Bi_{0.78}Sb_{0.22}$) are basically the same as that shown in Fig. 1(a), implying that the quality of the $Bi_{1-x}Sb_x$ films is not so much changed compared to the pristine Bi films. When the Sb concentration was increased to 32%, we could not obtain a clear 1×1 pattern even after the film thickness reached 50 Å (13 BL), as shown in Fig. 1(d). The features in Fig. 1(d) are similar to that of the rotationally disordered yet highly flat {012} oriented films of pure Bi.[16,17] The presence of high concentration of Sb may have some effect on the allotropic transformation from the {012} phase to the (001) phase,[16] but the precise mechanism is beyond the scope of the present work. As a result we can say that single-crystalline epitaxial $Bi_{1-x}Sb_x$ ultrathin alloy films can be prepared on Si(111)-7×7 in the range of $0\leq x<0.32$ and particularly in the region $0.07<x<0.22$ where the bulk topological insulator is predicted to be realized.

The core-level spectra of Sb 4*d* and Bi 5*d* were measured to confirm if the above stoichiometry estimated by the RHEED observation is correct. Figures 2(a) and 2(b) show the Sb 4*d* and Bi 5*d* spectra measured with $h\nu$=80 eV at normal emission for 43 Å (11 BL) thick $Bi_{0.92}Sb_{0.08}$ (a) and 39 Å (10 BL) thick $Bi_{0.84}Sb_{0.16}$ (b) ultrathin films, respectively. The blue (solid) and green (dotted) lines are the fits to the raw data using Voigt line shapes with reasonable spin-orbit splitting and branching ratio values. The composition of the film can be obtained by

$$\frac{\rho_{Bi}}{\rho_{Sb}} = \frac{I_{Bi}}{S_{Bi}} \Big/ \frac{I_{Sb}}{S_{Sb}}, \quad (1)$$

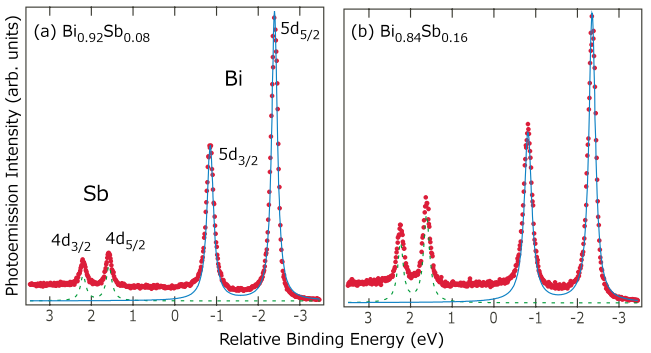

FIG. 2. (Color online) Core level photoemission spectra of Sb 4*d* and Bi 5*d* peaks for 43 Å (11 BL) thick $Bi_{0.92}Sb_{0.08}$ (a) and 39 Å (10 BL) thick $Bi_{0.84}Sb_{0.16}$ (b) ultrathin films measured at normal emission with $h\nu$=80 eV.

where ρ is the atomic density, I is the integrated peak intensity, and S is the atomic cross section. By using S_{Bi} =11.07 Mb and S_{Sb}=15.88 Mb,[18] $\frac{\rho_{Bi}}{\rho_{Sb}}$ is obtained as ~11.4 (a) and ~5.4 (b). These values are consistent with the estimation of $Bi_{0.92}Sb_{0.08}$ for (a) and $Bi_{0.84}Sb_{0.16}$ (b), respectively. Since the spot size of the photons (<1 mm in diameter) was much smaller than the sample size (typically 4 ×10 mm^2), we moved the beam position and investigated whether there was any inhomogeneity of the stoichiometry. It turned out that there was only about ±10% distribution around the mean value, indicating rather good homogeneity of the ultrathin $Bi_{1-x}Sb_x$ alloy films.

Next, we have tried to characterize the electronic structure of these films, namely the Fermi surface to extract the Z_2 topological number. Figures 3(a) and 3(b) show the results of the photoemission intensity at the Fermi level E_F for the 43 Å thick $Bi_{0.92}Sb_{0.08}$ (a) and 39 Å thick $Bi_{0.84}Sb_{0.16}$ (b) ultrathin films, respectively. They resemble that of the pure ultrathin Bi film;[19] a hexagonal electron pocket around the $\bar{\Gamma}$ point, hole lobes along the $\bar{\Gamma}-\bar{M}$ direction, and a needlelike electron pocket around the $\bar{M}$ point can be seen. All of the Fermi surface segments are composed of surface states. However, the Fermi wave number of each pocket has changed and this is the result of Sb alloying. In Ref. 6, the authors showed for bulk $Bi_{0.9}Sb_{0.1}$ that there are actually two separate bands that constitute the electron pocket near $\bar{M}$ which fulfilled the criterion of the nontrivial Z_2 topological number. In order to check whether a similar situation applies to the case of ultrathin alloy films, we have investigated the band dispersion near the $\bar{M}$ point in more detail. Figures 3(c) and 3(d) show the band dispersion obtained by energy and angle multidetections taken at $k_{\bar{\Gamma}-\bar{M}}$=0.60 $Å^{-1}$ in Fig. 3(a) and $k_{\bar{\Gamma}-\bar{M}}$=0.92 $Å^{-1}$ in Fig. 3(b), respectively. There are two clear bands in both images; the shallow one crossing E_F is the surface state and the band below with the linear dispersion is the bulk band.[6] Figures 3(e) and 3(f) show the raw photoemission spectra in 0.1° steps extracted from Figs. 3(c) and 3(d), respectively. To examine if the spectra contain two peaks near E_F, we have first compared them to the spectra near $\bar{\Gamma}$, as shown in Fig. 4(a). It can be seen that the peak width for the spectra around $\bar{M}$ is larger than those near $\bar{\Gamma}$,

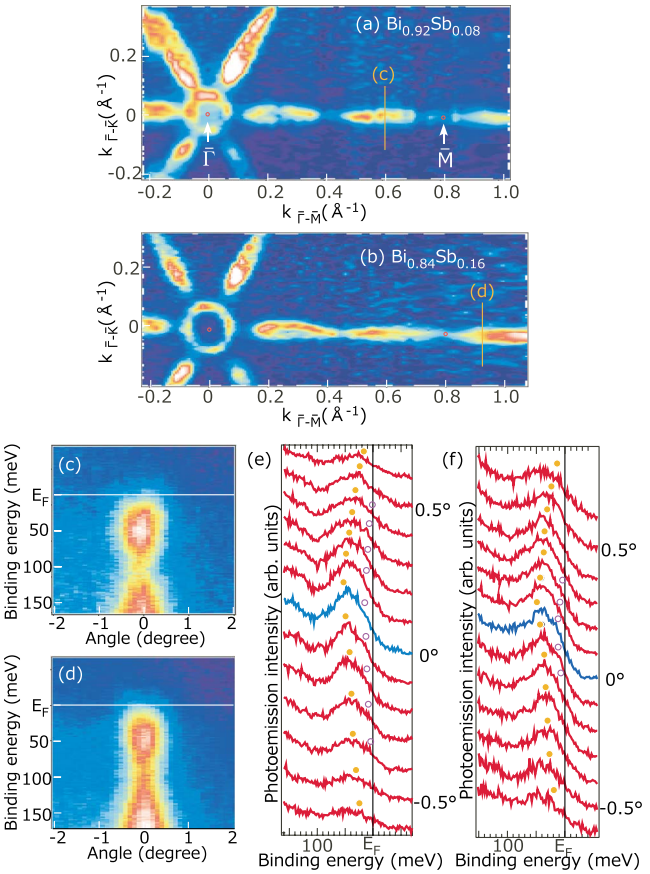

FIG. 3. (Color online) (a, b) Fermi surfaces of 43 Å thick $Bi_{0.92}Sb_{0.08}$ (a) and 39 Å thick $Bi_{0.84}Sb_{0.16}$ (b) ultrathin films. (c, d) $E-\theta$ band dispersions for the cuts shown in (a) and (b), respectively. (e, f) Energy distribution curves for the images shown in (c) and (d), respectively. The photon energy was $h\nu$=29 eV.

indicating the presence of two peaks. We have further performed a fitting procedure to the spectra to determine the energy positions with a convolution of the Fermi distribution function, Voigt line shapes for the two peaks and a linear background. The Gaussian linewidth was fixed to 20 meV (instrumental resolution) and the Lorentzian linewidth was 20–35 meV. Representative results of the fitting are shown in Figs. 4(b). For the spectra away from 0° such as the spectrum for −0.5° in Fig. 3(e), the peak width becomes smaller, indicating that one state has crossed the Fermi level [bottom spectrum of Fig. 4(a)]. Following the band dispersion shown by the filled and open circles in Figs. 3(e) and 3(f), the Fermi wave numbers for the two bands are determined as ~0.016 $Å^{-1}$ and ~0.030 $Å^{-1}$, respectively, in Fig. 3(e), and ~0.009 $Å^{-1}$ and ~0.026 $Å^{-1}$ in Fig. 3(f). Thus as in the case of single crystal bulk $Bi_{0.9}Sb_{0.1}$ (Ref. 6), the electron pocket around $\bar{M}$ is composed of two separate segments, which is shown schematically in Figs. 4(c) and 4(d). The topological number ν_0 is calculated by counting the number of Fermi surface arcs enclosing the time-reversal-invariant momenta (TRIM, $\bar{\Gamma}$, $\bar{M}_1$, $\bar{M}_2$, and $\bar{M}_3$).[1] From Fig. 4(d), there are seven Fermi surface segments enclosing the TRIM in total, one around $\bar{\Gamma}$ and two for each $\bar{M}$ point. Since seven is an odd number, the topological class of $Bi_{0.92}Sb_{0.08}$ and

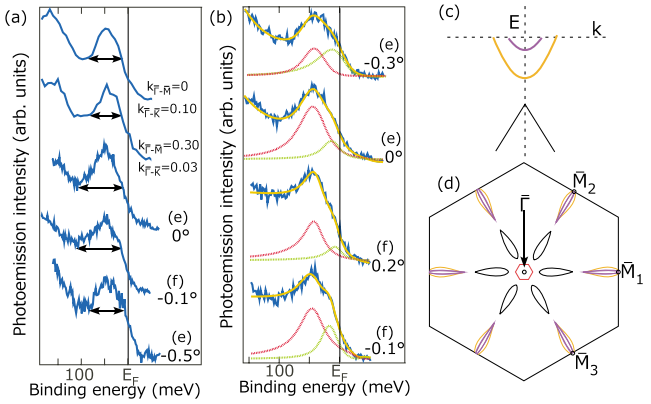

FIG. 4. (Color online) (a) Comparison of the peak width for the ARPES spectra near $\bar{\Gamma}$ and those shown in Figs. 3(e) and 3(f). The arrows show the width of the peak. (b) Representative results of the fitting for the spectra shown in Figs. 3(e) and 3(f). The red (dark) and green (light) curves show the states at higher and lower binding energies, respectively. (c) Schematic drawing of the band dispersion of Figs. 3(c)–3(f). (d) Schematic drawing of the Fermi surface shown in the surface Brillouin zone. The photon energy was $h\nu$ =29 eV.

$Bi_{0.84}Sb_{0.16}$ ultrathin films is nontrivial. We note that these ultrathin films are 3D TI. In Ref. 20, it was reported that when the film thickness is thinner than 6 BL (24 Å), the penetration depth of the surface states become comparable to the thickness and the surface-state band dispersion is modified compared to the thicker films and the semi-infinite crystal for pure Bi. Therefore the $Bi_{1-x}Sb_x$ films reported in the present work (>29 Å) is at the boundary of the 3D and 2D cases but still 3D.

Finally, we move on to the most important point: how do the surface states show up in the film property? For the case of pure Bi films, the surface-state contribution dominate the film conductivity when the thickness is 25 Å.[21] If the same situation is realized in $Bi_{1-x}Sb_x$, it would be an excellent platform to examine the nature of the topologically protected edge states as well as to flow dissipationless spin current. Since an energy gap is predicted to open for the bulk bands and they become insulating while the surface state is metallic, we can verify which is dominant (surface or bulk) by measuring the temperature dependence of the film conductivity. Figure 5 shows the temperature dependence of the two-dimensional resistivity measured by MFPP for 239 Å thick pure Bi (purple open circles), 239 Å thick $Bi_{0.9}Sb_{0.1}$ (blue filled diamonds), 98 Å thick $Bi_{0.9}Sb_{0.1}$ (green filled squares), and 29 Å thick $Bi_{0.9}Sb_{0.1}$ (orange filled circles) ultrathin films, respectively. Whereas the resistivity decreases upon cooling for the 239 Å pure Bi film, it increases in the case of a $Bi_{0.9}Sb_{0.1}$ film of the same thickness, showing that the bulk band energy gap has opened. When the film thickness is reduced, the temperature dependence of the film shows an insulator-to-metal transition for the 98 Å thick $Bi_{0.9}Sb_{0.1}$ film and a metallic behavior in the whole temperature range for the 29 Å thick $Bi_{0.9}Sb_{0.1}$ film. This metallic behavior clearly shows that the surface-state contribution is increasing when the film thickness is reduced. For the 98 Å thick film, there is a switching of the majority conduction

channel; from room temperature to 150 K, the bulk or the contribution inside the films dominate whereas below 150 K, the surface-state channel gives the largest contribution. Furthermore, we can say that for the 29 Å thick film, the film conductivity is solely determined by the surface states. Thus investigating the physical properties of the thinnest $Bi_{1-x}Sb_x$ alloy ultrathin films can indeed be directly related to the nature of the topological metals.

Additionally, we comment on the gap size of the alloy films. In the previous reports the observed energy gaps for the single crystal case was ~20 meV at maximum ($x \sim 0.15$ Ref. 22). However since the Fermi wavelength of Bi is 200–300 Å, which is larger or comparable to the alloy film thickness, the quantum size effect[23] (QSE) is expected to enlarge the band gap. To test this hypothesis, we have fitted the data points in the region of 100–300 K in Fig. 5 to a simple thermal activation-type function

$$\rho = \rho_0 \exp\left(\frac{E_g}{2k_B T}\right), \tag{2}$$

where ρ is the resistivity and E_g is the energy gap.[24] Due to the scattering of the data, the deduced value of E_g showed variation around 35–42 meV (the pink solid curve in Fig. 5 is the result for E_g=38 meV), which is three to four times larger than the energy gap of bulk $Bi_{0.9}Sb_{0.1}$ (~10 meV) reported in Ref. 22. For the 98 Å thick films, the same analysis revealed $E_g \sim 42-48$ meV (the pink solid line in Fig. 5 is for E_g=46 meV). Thus we can say that not only the surface/volume ratio is enhanced in these ultrathin films but also the bulk band gap is enlarged which are both favorable to investigate the intriguing properties of topological surface states.

Now let us compare the present results with recent reports for single crystals.[6,12] The values of residual resistivity ρ_{2D}^{res} (the resistivity extrapolated to T=0, red dotted lines in Fig. 5) are ~180, 300, and 550 Ω/□ for the 239, 98, and 29 Å thick $Bi_{0.9}Sb_{0.1}$ ultrathin films, respectively. This clearly shows thickness dependence and we speculate that the bulk or the film contribution is still present for the thicker films. This is also evidenced by the fact that ρ_{2D}^{res} for the single crystal cases are $\sim 3.0 \times 10^{-2}$ Ω/□ (0.1 mm thick, Ref. 12) and $\sim 1.0 \times 10^{-1}$ Ω/□ (1 mm thick, Ref. 6), which are much smaller than the values shown above. Even though bulk $Bi_{1-x}Sb_x$ is said to be a semiconductor, some 3D metallic components remain as shown in Refs. 12 and 22. At moderate temperature, the excitation of carriers with small energy gaps is the dominant conduction mechanism for these bulk materials. When the temperature becomes low enough that the semiconducting carriers freeze out, the metallic conduction shows up.[12] Even in the case of Ref. 6 in which the metallic behavior is not observed, the resistivity does not diverge and we speculate that this is due to the remaining metallicity. By reducing the thickness, the band gap enlarges (QSE) and leads to the absence of the metallic behavior at low temperature of the bulk (film) carriers presumably due to the suppressed surface-bulk coupling (239 Å thick film). As the film thickness is further reduced (98 Å), an insulator-to-metal transition is found again; however this is different

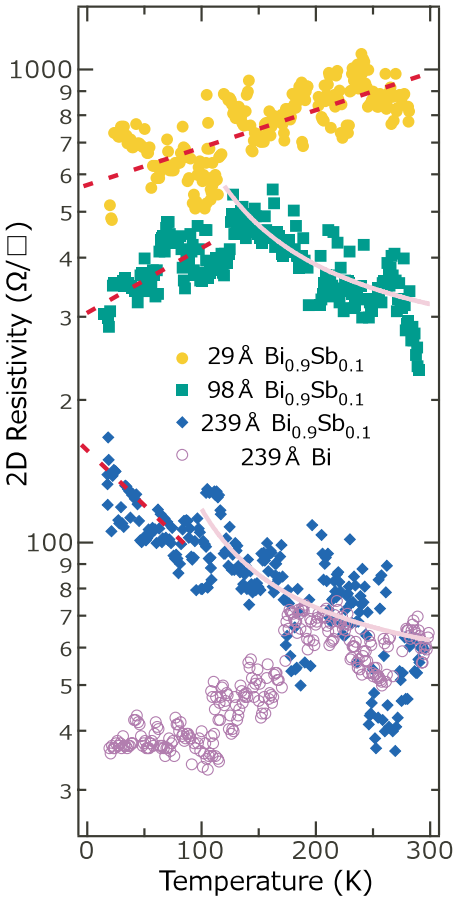

FIG. 5. (Color online) The temperature dependence of two-dimensional resistivity for 239 Å thick pure Bi (purple open circles), 239 Å thick $Bi_{0.9}Sb_{0.1}$ (blue filled diamonds), 98 Å thick $Bi_{0.9}Sb_{0.1}$ (green filled squares), and 29 Å thick $Bi_{0.9}Sb_{0.1}$ (orange filled circles) ultrathin films measured by *in situ* micro-four-point probe method. The pink solid lines are the least-square linear fits to Eq. (2) and the red solid lines show the linear extrapolation to T=0.

from that found in single crystals and shows *the change from a bulk (film) conductivity to a surface-state-dominant conductivity*. By reducing the film thickness even further (29 Å), we find that the film contribution becomes negligible compared to the surface-state conductivity and thus results in the metallic behavior in the whole temperature range. Since ρ_{2D}^{res} in the bulk single crystal is $\sim 10^{-4}$ times smaller than that of the surface states,[25] it is impossible to detect the surface-state conductivity using them even at low temperature. Similar finding has been reported for pure Bi.[26] As a consequence, these ultrathin films are ideal systems for investigation of the properties of TI.

In conclusion, we have performed RHEED observations, ARPES, and conductivity measurements on ultrathin $Bi_{1-x}Sb_x$ alloy films on Si(111). We found that epitaxial films as thin as 30 Å can be prepared. The Fermi surface formed by the surface states showed that the films possess nontrivial Z_2 topological numbers. Finally we observed a crossover from an insulating to a surface-state dominant metallic conduction as the film thickness was reduced and the bulk band

gap was enlarged compared to the bulk case. Our analyses reveal that it is impossible to measure the surface-state contribution with bulk crystals and the surface/volume ratio needs to be enhanced drastically to investigate the topological-metal conductivity.

This work has been supported by Grants-In-Aid from Japanese Society for the Promotion of Science. The ARPES experiments were performed under the proposal numbers of PF 2007G578 and UVSOR 21-524.

*hirahara@surface.phys.s.u-tokyo.ac.jp
†Present address: HSRC, Hiroshima University, Higashi-Hiroshima 739-0046, Japan.

[1] L. Fu and C. L. Kane, Phys. Rev. B **76**, 045302 (2007).
[2] C. L. Kane and E. J. Mele, Phys. Rev. Lett. **95**, 146802 (2005).
[3] C. Wu, B. A. Bernevig, and S.-C. Zhang, Phys. Rev. Lett. **96**, 106401 (2006).
[4] X.-L. Qi, R. Li, J. Zang, and S.-C. Zhang, Science **323**, 1184 (2009).
[5] L. Fu and C. L. Kane, Phys. Rev. Lett. **100**, 096407 (2008).
[6] D. Hsieh, D. Qian, L. Wray, Y. Xia, Y. S. Hor, R. J. Cava, and M. Z. Hasan, Nature (London) **452**, 970 (2008).
[7] A. Nishide, A. A. Taskin, Y. Takeichi, T. Okuda, A. Kakizaki, T. Hirahara, K. Nakatsuji, F. Komori, Y. Ando, and I. Matsuda, Phys. Rev. B. **81**, 041309(R) (2010).
[8] D. Hsieh, Y. Xia, L. Wray, D. Qian, A. Pal, J. H. Dil, J. Osterwalder, F. Meier, G. Bihlmayer, C. L. Kane, Y. S. Hor, R. J. Cava, and M. Z. Hasan, Science **323**, 919 (2009).
[9] Y. Xia, D. Qian, D. Hsieh, L. Wray, A. Pal, H. Lin, A. Bansil, D. Grauer, Y. S. Hor, R. J. Cava, and M. Z. Hasan, Nat. Phys. **5**, 398 (2009).
[10] Y. L. Chen, J. G. Analytis, J.-H. Chu, Z. K. Liu, S.-K. Mo, X. L. Qi, H. J. Zhang, D. H. Lu, X. Dai, Z. Fang, S. C. Zhang, I. R. Fisher, Z. Hussain, and Z.-X. Shen, Science **325**, 178 (2009).
[11] D. Hsieh, Y. Xia, D. Qian, L. Wray, J. H. Dil, F. Meier, J. Osterwalder, L. Patthey, J. G. Checkelsky, N. P. Ong, A. V. Fedrov, H. Lin, A. Bansil, D. Grauer, Y. S. Hor, R. J. Cava, and M. Z. Hasan, Nature (London) **460**, 1101 (2009).
[12] A. A. Taskin and Y. Ando, Phys. Rev. B **80**, 085303 (2009).
[13] C.-X. Liu, H. Zhang, B. Yan, X. Qi, T. Frauenheim, X. Dai, Z. Fang, and S.-C. Zhang, Phys. Rev. B **81**, 041307(R) (2010); J. Linder, T. Yokoyama, and A. Sudbø, *ibid.* **80**, 205401 (2009).
[14] T. Tanikawa, I. Matsuda, R. Hobara, and S. Hasegawa, e-J. Surf. Sci. Nanotechnol. **1**, 50 (2003).
[15] V. G. Lifshits, A. A. Saranin, and A. V. Zotov, *Surface Phases on Silicon* (Wiley, New York, 1994).
[16] T. Nagao, J. T. Sadowski, M. Saito, S. Yaginuma, Y. Fujikawa, T. Kogure, T. Ohno, Y. Hasegawa, S. Hasegawa, and T. Sakurai, Phys. Rev. Lett. **93**, 105501 (2004).
[17] T. Nagao, T. Doi, T. Sekiguchi, and S. Hasegawa, Jpn. J. Appl. Phys., Part 1 **39**, 4567 (2000).
[18] J. J. Yeh and I. Lindau, At. Data Nucl. Data Tables **32**, 1 (1985).
[19] T. Hirahara, T. Nagao, I. Matsuda, G. Bihlmayer, E. V. Chulkov, Yu. M. Koroteev, P. M. Echenique, M. Saito, and S. Hasegawa, Phys. Rev. Lett. **97**, 146803 (2006).
[20] Yu. M. Koroteev, G. Bihlmayer, E. V. Chulkov, and S. Blügel, Phys. Rev. B **77**, 045428 (2008).
[21] T. Hirahara, I. Matsuda, S. Yamazaki, N. Miyata, S. Hasegawa, and T. Nagao, Appl. Phys. Lett. **91**, 202106 (2007).
[22] B. Lenoir, M. Cassart, J.-P. Michenaud, H. Scherrer, and S. Scherrer, J. Phys. Chem. Solids **57**, 89 (1996).
[23] T. Hirahara, T. Nagao, I. Matsuda, G. Bihlmayer, E. V. Chulkov, Yu. M. Koroteev, and S. Hasegawa, Phys. Rev. B **75**, 035422 (2007).
[24] We have not included the data points below 100 K in the fitting because it can be anticipated that the contribution from the surface states will make the apparent gap size smaller. Indeed, we could not obtain a reasonable fitting curve when we considered all the data points shown in Fig. 5.
[25] This difference is too large to be ascribed to the better surface quality of the bulk single crystals.
[26] J. W. Wells, K. Handrup, J. F. Kallehauge, L. Gammelgaard, P. Bøggild, M. B. Balslev, J. E. Hansen, P. R. E. Petersen, and Ph. Hofmann, J. Appl. Phys. **104**, 053717 (2008).